Electronic Supplementary Information (ESI)

Gold-Doped Silver Nanocluster $[Au_3Ag_{38}(SCH_2Ph)_{24}X_5]^{2-}$ (X= Cl or Br)

Zhi Wang,[a] Ravithree Senanayake,[b] Christine M. Aikens,[b] Wen-Miao Chen,[a] Chen-Ho Tung,[a] Di Sun*,[a]

[a]*Key Lab of Colloid and Interface Chemistry, Ministry of Education, School of Chemistry and Chemical Engineering, Shandong University, Jinan, 250100, P. R. China. E-mail: dsun@sdu.edu.cn.*
[b] *Department of Chemistry, Kansas State University, Manhattan, Kansas 66506, United States.*

Experiment details

All reagents and solvents employed were commercially available and used as received without further purification. The emission spectra was measured with a lumina fluorescence spectrometer (Thermo Scientific). The solution UV-Vis absorption spectrum was measured on UV-Vis spectrophotometer (Evolution 220, ISA-220 accessory, Thermo Scientific). IR spectra were recorded on a PerkinElmer Spectrum Two in the frequency range of 4000-400 cm^{-1}. Elemental analyses for C, and H were performed on a PerkinElmer 2400 CHN elemental analyzer and, for Ag and Au were performed on a PLASMASPEC (I) ICP atomic emission spectrometer. Morphologies were characterized by high-resolution transmission electron microscopy at 200 kV (JEM-2100, JEOL Ltd., Tokyo, Japan). Energy-dispersive X-ray spectrum was measured using an SU-8010 field emission scanning electron microscope (FESEM; Hitachi Ltd., Tokyo, Japan) equipped with an Oxford-Horiba Inca XMax50 energy-dispersive X-ray (EDX; Oxford Instruments Analytical, High Wycombe, England). Differential pulse voltammetry (DPV) was conducted on an electrochemical work station model CHI-660 with a standard three-electrode system (glassy carbon working, Pt wire auxiliary, and Ag/Ag^{+} reference); study was performed on CH_2Cl_2 solutions containing 0.1 M $NBu^{n}_4PF_6$ as supporting electrolyte.

X-ray Crystallography

Single crystal of complex **1** of appropriate dimensions was chosen under an optical microscope and quickly coated with high vacuum grease (Dow Corning Corporation) to prevent decomposition and one was mounted on a glass fiber for data collection on a Bruker Apex II CCD diffractometer equipped with graphite-monochromated Mo Kα radiation (λ = 0.71073 Å) at 123 K. A preliminary orientation matrix and unit cell parameters were determined from 3 runs of 12 frames each, each frame corresponds to a 0.5° scan for 5 s, followed by spot integration and least-squares refinement. For the full structure of **1**, data were measured using ω scans of 2° per frame for 30 s until a complete hemisphere had been collected. Cell parameters were retrieved using SMART software and refined with SAINT on all observed reflections. Data reduction was performed with the SAINT software and corrected for Lorentz and polarization effects. Absorption corrections were applied with the program SADABS. The highest possible space group was chosen. The structure was solved by direct methods using SHELXS-97 and refined on F^2 by full-matrix least-squares procedures with SHELXL-97. Atoms were located from iterative examination of difference *F*-maps following least squares refinements of the preceding models. Hydrogen atoms were placed in calculated positions and included as riding atoms with isotropic displacement parameters 1.2-1.5 times U_{eq} of the attached C atoms. All structures were examined using the Addsym subroutine of PLATON to ensure that no additional symmetry could be applied to the models. Pertinent crystallographic data collection and refinement parameters are collated in Table S1. Selected bond lengths and angles are collated in Table S2.

Synthesis of Au(PPh_2Py)Cl

Au(PPh_2Py)Cl was synthesized using a improved process of a previous report reference (N. Baenziger, W. Bennett and D. Soborofe, *Acta Cryst.* **1976**, *B32*, 962-963.) Typically, 1.469 g PPh_2Py was dissloved in 10ml ethanol (99.7%) under stirring to afford a clear by heating 50 ^oC, then 1 g $HAuCl_4 \cdot 4H_2O$ (Au > 47%) in 20 mL ethanol was added into above solution, white precipitates formation when mixed together. Before filtrated the mixture was stirred another 2 h to obtain the white fiber-like Au(PPh_2Py)Cl microcrystals.

Synthesis of cluster 1.

In a 100 mL flask, 6 mg Au(PPh_2Py)Cl was added to 15 mL dichloromethanol. A solution of 34 mg $AgNO_3$ in 5 mL methanol was then added to the flask and the solution was cooled to 0 ^oC. To this solution, 26 μL phenylacetylene and 28 μL benzenemethanethiol were added that produced a clear yellow solution. After 3 mg PPh_4Br was added in and stirred for 30 min, the clear yellow solution turned opaque, then 4 mg of $NaBH_4$ in 1 mL of ice-cold water with 25 μL triethylamine were added dropwise under vigorous stirring (~1500 rpm), the solution turned dark red quickly and kept the speed for another 12 h. Then the mixture in organic phase was washed three times with water and dried by rotary evaporation to give a dark products, which was dissolved in $CHCl_3$-$C_2H_2Cl_4$ mixed solvents. The resulting solution was filtered through a syringe filter with pore size 450 nm and was subject to diffusion with hexane to obtain black rhombus crystals after ca. 18 days. Elemental analysis for vacuum dried **1** ($C_{216}H_{208}Au_3Ag_{38}S_{24}P_2Br_{1.9}Cl_{3.1}$), calcd (%): Ag, 47.7; Au, 6.9; C, 30.2; H, 2.4, found: Ag, 47.2; Au, 7.2; C, 30.5; H, 2.2. IR: 2919 (w), 1727 (w), 1600 (w), 1497 (m), 1440 (m), 1335 (m), 1108 (m), 1020 (m), 689 (s), 524 (s) cm^{-1}.

Table S1: Crystal Data Collection and Structure Refinement for 1.

Empirical formula	$C_{226}H_{218}Ag_{38}Au_3Br_{1.9}Cl_{25.1}P_2S_{24}$
Formula weight	9496.96
Temperature/K	120.15
Crystal system	monoclinic
Space group	P21/c
a/Å	35.113(4)
b/Å	34.407(4)
c/Å	24.991(3)
α/°	90
β/°	100.595(2)
γ/°	90
Volume/Å^3	29678(6)
Z	4
ρcalcg/cm3	2.125
μ/mm-1	4.619
F(000)	18017.0
Crystal size/mm3	0.06 × 0.05 × 0.03
Radiation	Mo Kα (λ = 0.71073)
2Θ range for data collection/°	4.854 to 50
Index ranges	-38 ⩽ h ⩽ 41, -38 ⩽ k ⩽ 40, -29 ⩽ l ⩽ 28
Reflections collected	121553
Independent reflections	51586 [R_{int} = 0.0652, R_{sigma} = 0.1179]
Data/restraints/parameters	51586/883/2696
Goodness-of-fit on F2	1.059
Final R indexes [I>=2σ (I)]	R_1 = 0.0999, wR2 = 0.2695
Final R indexes [all data]	R_1 = 0.1507, wR2 = 0.2929
Largest diff. peak/hole / e Å^{-3}	3.44/-2.11

Table S2: Selected bond lengths (Å) and angles (°) in 1.

Ag1—Ag3	2.894 (2)	Ag18—Ag19	2.943 (2)
Ag1—Ag10	2.863 (2)	Ag18—Ag29	2.991 (2)
Ag1—Ag5	3.173 (2)	Ag18—Au1	2.8492 (18)
Ag1—S2	2.471 (7)	Ag18—Br2	2.802 (5)
Ag1—S5	2.502 (6)	Ag18—S13	2.671 (7)
Ag1—S22	2.549 (6)	Ag19—Ag20	3.011 (2)
Ag2—Ag10	2.821 (3)	Ag19—Ag21	3.066 (2)
Ag2—Ag6	2.888 (2)	Ag19—Ag29	2.879 (2)
Ag2—S1	2.451 (7)	Ag19—Ag38	2.974 (2)
Ag2—S2	2.639 (7)	Ag19—Ag39	3.262 (2)
Ag2—S12	2.519 (7)	Ag19—Au1	2.8618 (17)
Ag3—Ag10	3.078 (2)	Ag19—S19	2.820 (6)
Ag3—Ag5	2.914 (2)	Ag19—S24	2.760 (5)
Ag3—Ag6	2.998 (2)	Ag20—Ag21	2.865 (2)
Ag3—Ag7	2.945 (2)	Ag20—Ag39	3.081 (2)
Ag3—Ag9	2.899 (2)	Ag20—Br3	2.567 (5)
Ag3—Ag37	2.901 (2)	Ag20—S18	2.590 (6)
Ag3—Au1	2.7792 (18)	Ag20—S19	2.421 (6)
Ag3—Br5	2.728 (4)	Ag21—Ag22	2.987 (2)
Ag3—S22	2.544 (6)	Ag21—Ag29	2.9343 (19)
Ag10—Ag5	2.924 (2)	Ag21—Ag39	2.848 (2)
Ag10—Ag6	2.868 (2)	Ag21—Au1	2.7695 (16)
Ag10—Ag14	2.753 (2)	Ag21—Au2	2.7468 (16)
Ag10—Au1	2.8489 (17)	Ag22—Ag23	2.947 (2)
Ag10—Br4	3.013 (3)	Ag22—Ag24	3.113 (3)
Ag10—S2	2.507 (6)	Ag22—Ag25	3.034 (2)
Ag5—Ag9	2.888 (2)	Ag22—Ag26	3.025 (2)
Ag5—Ag14	2.828 (2)	Ag22—Au2	2.8360 (18)
Ag5—Ag15	2.904 (2)	Ag22—Br3	2.805 (5)
Ag5—Ag21	2.897 (2)	Ag22—S16	2.681 (6)
Ag5—Au1	2.8376 (18)	Ag23—Ag26	2.884 (2)
Ag5—S5	2.474 (5)	Ag23—Ag39	3.036 (2)
Ag6—Ag7	3.166 (2)	Ag23—S15	2.503 (6)
Ag6—Ag16	2.762 (3)	Ag23—S16	2.574 (6)
Ag6—Ag18	3.003 (2)	Ag23—S18	2.449 (6)
Ag6—Au1	2.7634 (19)	Ag24—Ag25	2.759 (2)
Ag6—Br5	2.690 (4)	Ag24—S9	2.400 (6)
Ag6—S12	2.685 (7)	Ag24—S16	2.355 (6)
Ag7—Ag8	3.084 (2)	Ag25—Ag26	3.230 (2)
Ag7—Ag9	2.956 (2)	Ag25—Ag34	3.006 (2)

Ag7—Ag17	2.961 (2)	Ag25—Au2	2.7572 (19)
Ag7—Ag18	3.054 (2)	Ag25—Br1	2.676 (4)
Ag7—Ag19	2.938 (2)	Ag25—S9	2.656 (6)
Ag7—Au1	2.7430 (17)	Ag26—Ag27	2.989 (2)
Ag7—Br5	2.852 (4)	Ag26—Ag28	2.938 (2)
Ag7—S23	2.491 (5)	Ag26—Ag34	2.886 (2)
Ag8—Ag9	2.972 (2)	Ag26—Ag39	2.933 (2)
Ag8—Ag37	3.200 (2)	Ag26—Au2	2.7435 (18)
Ag8—S19	2.403 (6)	Ag26—Br1	2.770 (4)
Ag8—S21	2.387 (6)	Ag26—S15	2.514 (6)
Ag8—S23	2.827 (6)	Ag27—Ag28	3.037 (2)
Ag9—Ag15	3.173 (2)	Ag27—Ag33	3.101 (3)
Ag9—Ag19	3.208 (2)	Ag27—S10	2.412 (6)
Ag9—Ag20	3.190 (2)	Ag27—S14	2.591 (6)
Ag9—Ag21	2.790 (2)	Ag27—S15	2.546 (6)
Ag9—Ag37	3.044 (2)	Ag28—Ag29	2.822 (2)
Ag9—Au1	2.7919 (17)	Ag28—Ag31	3.212 (2)
Ag9—S20	2.521 (5)	Ag28—Ag32	2.918 (2)
Ag4—Ag11	3.202 (5)	Ag28—Ag33	3.185 (2)
Ag4—Br4	2.856 (5)	Ag28—Ag34	2.942 (2)
Ag4—S5	2.489 (7)	Ag28—Ag38	3.212 (2)
Ag4—S7	2.451 (8)	Ag28—Ag39	3.137 (2)
Ag11—Ag12	2.861 (3)	Ag28—Au2	2.8546 (18)
Ag11—Ag25	2.924 (2)	Ag28—S11	2.532 (6)
Ag11—S6	2.648 (7)	Ag28—S14	2.760 (6)
Ag11—S7	2.441 (7)	Ag29—Ag32	2.904 (2)
Ag11—S9	2.506 (7)	Ag29—Ag38	2.885 (2)
Ag12—Ag14	2.761 (2)	Ag29—Ag39	2.993 (2)
Ag12—Ag25	2.830 (2)	Ag29—Au1	2.7407 (15)
Ag12—Ag32	2.949 (2)	Ag29—Au2	2.7815 (17)
Ag12—Ag34	3.157 (2)	Ag31—Ag32	2.898 (2)
Ag12—Ag35	2.899 (2)	Ag31—Br2	2.654 (4)
Ag12—Au2	2.8782 (18)	Ag31—S3	2.453 (6)
Ag12—Br4	3.049 (4)	Ag31—S11	2.448 (6)
Ag12—S6	2.497 (6)	Ag32—Ag34	2.884 (2)
Ag14—Ag32	2.832 (2)	Ag32—Ag35	3.292 (2)
Ag14—Au1	2.8277 (17)	Ag32—Au2	2.7855 (18)
Ag14—Au2	2.8094 (17)	Ag32—S4	2.455 (6)
Ag14—Br4	2.719 (3)	Ag33—Ag34	2.939 (3)
Ag15—Ag21	3.116 (2)	Ag33—S8	2.444 (6)
Ag15—Br3	2.716 (5)	Ag33—S10	2.409 (7)
Ag15—S17	2.442 (6)	Ag33—S11	2.615 (6)
Ag15—S20	2.471 (6)	Ag34—Ag35	2.874 (2)

Ag16—Ag18	3.190 (3)	Ag34—Au2	2.7667 (18)
Ag16—S12	2.367 (7)	Ag34—Br1	2.780 (4)
Ag16—S13	2.323 (7)	Ag34—S8	2.528 (6)
Ag17—Ag18	2.921 (2)	Ag35—S4	2.579 (6)
Ag17—Ag19	3.027 (2)	Ag35—S6	2.471 (7)
Ag17—S13	2.599 (6)	Ag35—S8	2.505 (7)
Ag17—S23	2.459 (6)	Ag36—S1	2.395 (7)
Ag17—S24	2.411 (6)	Ag36—S4	2.452 (7)
Ag37—S22	2.488 (6)	Ag37—S20	2.612 (6)
Ag38—Br2	2.738 (5)	Ag37—S21	2.448 (6)
Ag38—S24	2.473 (6)	Ag38—Ag39	2.917 (2)
Ag39—S18	2.574 (6)	Ag38—S14	2.418 (6)
Ag39—Au2	2.8272 (17)		
S2—Ag1—S5	124.7(2)	S2—Ag1—S22	127.8(2)
S5—Ag1—S22	105.6(2)	S1—Ag2—S2	107.6(2)
S1—Ag2—S12	124.7(2)	S12—Ag2—S2	118.8(3)
S22—Ag3—Br5	105.89(17)	S2—Ag10—Br4	101.50(17)
S12—Ag6—Br5	99.11(19)	S23—Ag7—Br5	103.13(16)
S19—Ag8—S23	87.07(19)	S21—Ag8—S19	161.7(2)
S21—Ag8—S23	110.3(2)	S5—Ag4—Br4	93.9(2)
S7—Ag4—Br4	114.5(3)	S7—Ag4—S5	139.7(3)
S7—Ag11—S6	102.9(3)	S7—Ag11—S9	130.3(3)
S9—Ag11—S6	118.5(2)	S6—Ag12—Br4	102.09(17)
S17—Ag15—Br3	107.76(18)	S17—Ag15—S20	144.19(19)
S20—Ag15—Br3	103.87(16)	S13—Ag16—S12	168.5(3)
S23—Ag17—S13	105.3(2)	S24—Ag17—S13	122.7(2)
S24—Ag17—S23	131.5(2)	S13—Ag18—Br2	94.82(17)
S24—Ag19—S19	93.99(17)	Br3—Ag20—S18	93.71(17)
S19—Ag20—Br3	139.28(19)	S19—Ag20—S18	117.6(2)
S18—Ag23—S15	124.9(2)	S18—Ag23—S16	126.6(2)
S16—Ag24—S9	169.4(2)	S9—Ag25—Br1	99.57(18)
S15—Ag26—Br1	102.80(16)	S10—Ag27—S14	134.6(2)
S10—Ag27—S15	135.3(2)	S15—Ag27—S14	88.00(18)
S11—Ag28—S14	106.28(18)	S3—Ag31—Br2	107.32(17)
S11—Ag31—S3	140.79(19)	S8—Ag33—S11	111.5(2)
S10—Ag33—S8	140.6(2)	S10—Ag33—S11	106.9(2)
S8—Ag34—Br1	102.64(18)	S6—Ag35—S4	118.1(2)
S6—Ag35—S8	131.0(2)	S8—Ag35—S4	108.8(2)
S1—Ag36—S4	155.4(2)	S21—Ag37—S20	110.0(2)
S21—Ag37—S22	143.9(2)	S22—Ag37—S20	104.95(19)
S14—Ag38—Br2	122.38(17)	S14—Ag38—S24	133.61(19)
S24—Ag38—Br2	88.12(16)		

Table S3. The transitions corresponding to the significant peaks in the $Au_3Ag_{38}(SCH_3)_{24}X_5]^{2-}$ spectrum. This also shows the oscillator strength, peak position, the corresponding value in nm, weights and transition dipole moments.

f (oscillator strength)	eV	nm	transitions	Weight	Transition dipole moment		
					x	y	z
0.009155	1.4250	870.1	HOMO-LUMO+1	0.8443	2.9032	0.2053	0.0384
			HOMO-1 -LUMO	0.0619	0.2707	0.3268	-0.0258
			HOMO-1 - LUMO+3	0.0411	-0.8175	-0.2206	-0.0285
0.01245	1.6281	761.5	HOMO-1 - LUMO+3	0.8148	3.4044	0.9186	0.1187
			HOMO-2 -LUMO	0.1207	-1.3075	-1.2794	0.1118
			HOMO-2 -LUMO+3	0.0198	-0.6295	0.1662	-0.0218
			HOMO -LUMO+1	0.0166	0.3809	0.0269	0.005
0.04021	2.1012	590.1	HOMO-2 -LUMO+4	0.6388	-0.2148	-0.6111	-1.0813
			HOMO - LUMO+5	0.0725	0.7303	0.6094	0.1234
			HOMO-8 -LUMO+3	0.0607	-0.1099	-0.1461	0.0079
			HOMO-2 -LUMO+3	0.0254	0.6263	-0.1654	0.0217
			HOMO-2 - LUMO	0.0213	0.4835	0.4731	-0.0413
			HOMO-2 - LUMO+2	0.0205	0.3437	0.3476	-0.0462
0.06835	2.1819	568.2	HOMO-9 -LUMO	0.3862	-0.3836	-0.2597	-0.0157
			HOMO-10 - LUMO	0.0912	-0.0275	0.2059	-0.2435
			HOMO-7 -LUMO+2	0.0687	0.1585	-0.0246	-0.0407
			HOMO-8 -LUMO	0.0594	-0.1067	-0.1419	0.0077
			HOMO - LUMO+5	0.0461	-0.5719	-0.4772	-0.0966
			HOMO-2 -LUMO+4	0.0367	-0.0505	-0.1437	-0.2542
			HOMO-2 -LUMO	0.0239	-0.5029	-0.4921	0.043
			HOMO-6 -LUMO+3	0.0193	0.1259	0.0261	0.0464
			HOMO - LUMO+6	0.0179	0.2149	-0.1344	-0.0756
			HOMO-2 -LUMO+2	0.0162	-0.3	-0.3034	0.0403
0.01758	2.5312	489.8	HOMO-14 - LUMO+3	0.2055	0.0223	0.2247	-0.0551
			HOMO-21 - LUMO	0.1578	0.0114	0.2224	0.1152
			HOMO-13 - LUMO+3	0.0835	0.0598	-0.1583	-0.0539
			HOMO-16 - LUMO+2	0.0528	0.0828	0.1468	0.021
			HOMO-4 - LUMO+5	0.05	-0.0582	-0.3031	0.2706
0.01249	2.5367	488.8	HOMO-16 -LUMO+2	0.2397	-0.1763	-0.3126	-0.0446
			HOMO-22 -LUMO	0.1724	-0.0059	0.1167	0.3368
			HOMO-21 - LUMO	0.0567	0.0068	0.1332	0.069
			HOMO-2 - LUMO+6	0.0545	-0.1809	0.0833	0.1425
0.03307	2.5652	483.3	HOMO-17 -LUMO+2	0.1185	0.0209	-0.0356	-0.077

			HOMO-8 - LUMO+4	0.1029	0.0967	0.353	-0.0779
			HOMO-22 -LUMO	0.0919	-0.0043	0.0847	0.2446
			HOMO-4 -LUMO+5	0.0887	-0.0771	-0.4011	0.3582
			HOMO-21 -LUMO	0.0845	-0.0083	-0.1616	-0.0837
0.02628	2.5919	478.4	HOMO-2 -LUMO+6	0.3573	-0.4582	0.2109	0.3608
			HOMO-19 -LUMO+2	0.112	-0.1123	-0.1246	-0.2579
			HOMO- 23 -LUMO	0.0748	-0.1861	-0.0917	-0.0126
			HOMO- LUMO+10	0.0702	0.1549	-0.1503	-0.1531
0.01082	2.5988	477.1	HOMO-19 - LUMO+2	0.2931	0.1814	0.2012	0.4166
			HOMO-8 - LUMO+4	0.2823	0.159	0.5808	-0.1282
			HOMO-20 -LUMO+2	0.2322	0.1555	-0.2546	-0.261
0.02879	2.6208	473.1	HOMO-20 -LUMO+2	0.2403	-0.1575	0.2579	0.2644
			HOMO-24 -LUMO	0.1564	0.1147	0.2966	0.0294
			HOMO-21 -LUMO+2	0.0946	0.0993	-0.2601	-0.1402
			HOMO - LUMO+10	0.0678	-0.1515	0.1469	0.1497
			HOMO-8 - LUMO+4	0.0554	0.0702	0.2562	-0.0565
0.01486	2.6231	472.7	HOMO-9 - LUMO+4	0.6687	-0.1908	-0.3848	0.5042
			HOMO-22 - LUMO+1	0.0703	0.0185	0.0624	0.0492
			HOMO-20 -LUMO+2	0.0557	-0.0758	0.1241	0.1272
0.01962	2.6794	462.7	HOMO-17 - LUMO+3	0.2263	0.0353	0.2482	-0.0828
			HOMO-22 -LUMO+2	0.2129	0.0149	-0.0476	0.4804
			HOMO-21 - LUMO+2	0.1434	-0.1209	0.3167	0.1707
0.01242	2.6990	459.4	HOMO-2 - LUMO+7	0.2327	-0.1284	0.2804	-0.0849
			HOMO-6 - LUMO+5	0.2293	-0.2286	0.2915	-0.1253
0.02489	2.7403	452.4	HOMO-20 -LUMO+3	0.3821	-0.1238	-0.1364	0.0773
			HOMO-25 -LUMO+1	0.0878	-0.1124	-0.1354	-0.0464

Fig. S1: TDDFT optical absorption spectrum for $[Au_4Ag_{37}(SCH_3)_{24}Br_5]^{2-}$

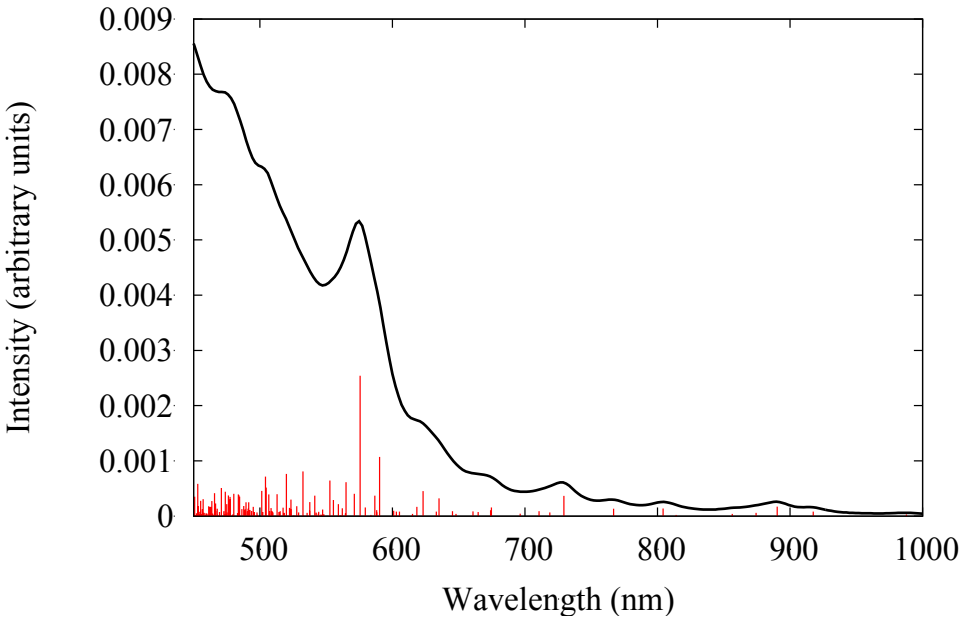

Fig. S2: TDDFT optical absorption spectrum for $[Au_2Ag_{39}(SCH_3)_{24}Br_5]^{2-}$

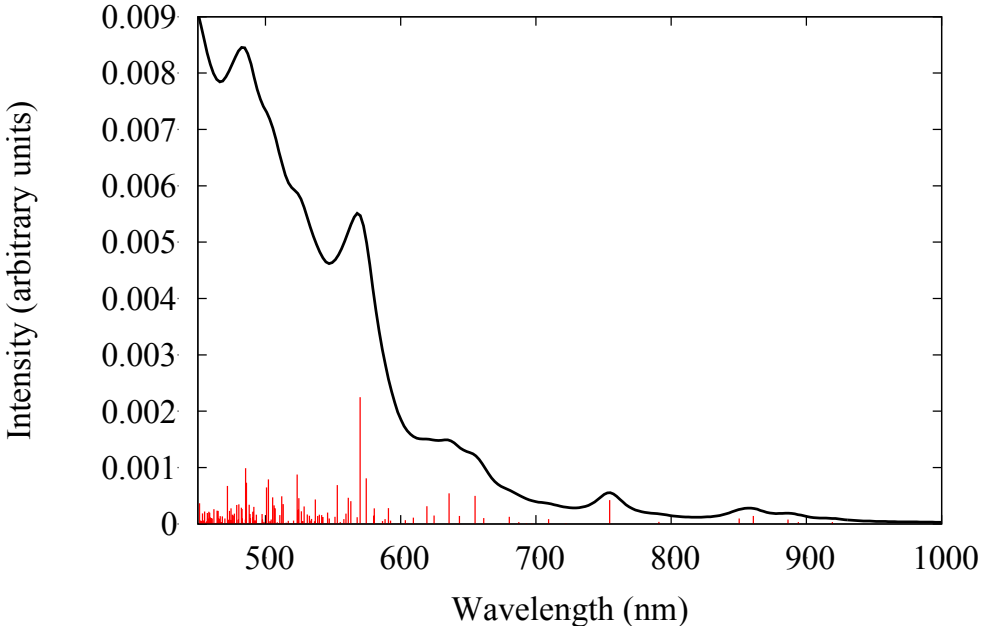

Fig. S3: The IR spectra of 1

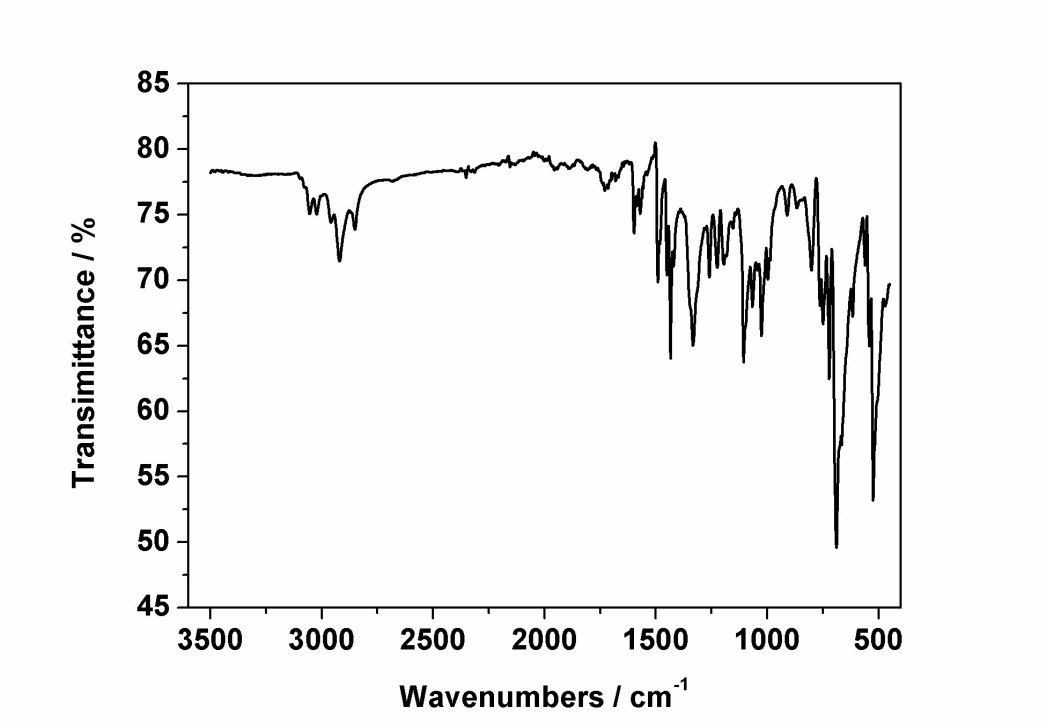

Fig. S4: The high-resolution TEM (HRTEM) images of 1.

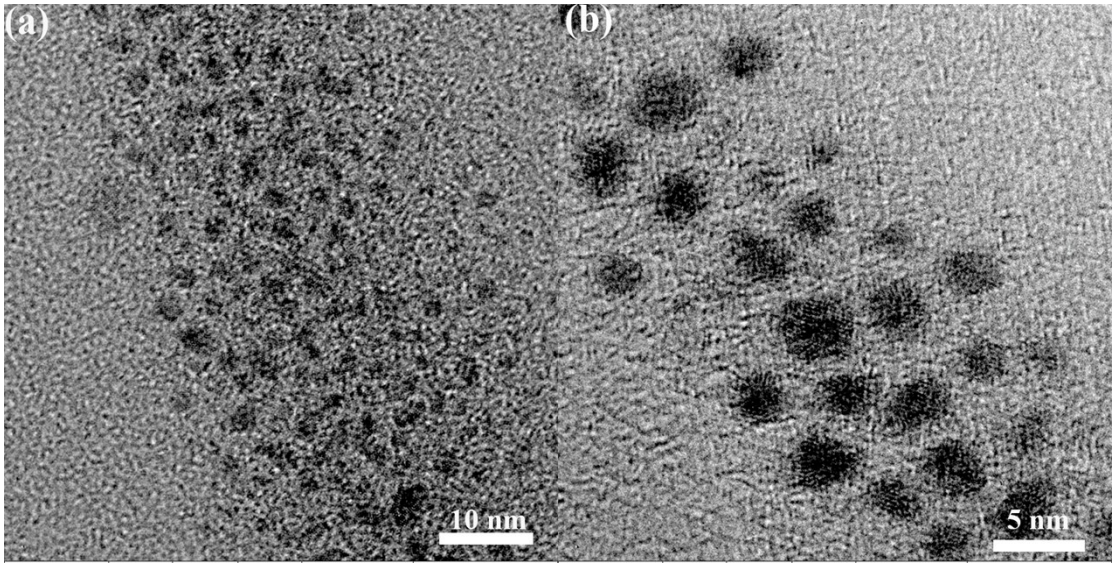

Fig. S5: Energy dispersive X-ray spectra (EDS) mapping of selected element.

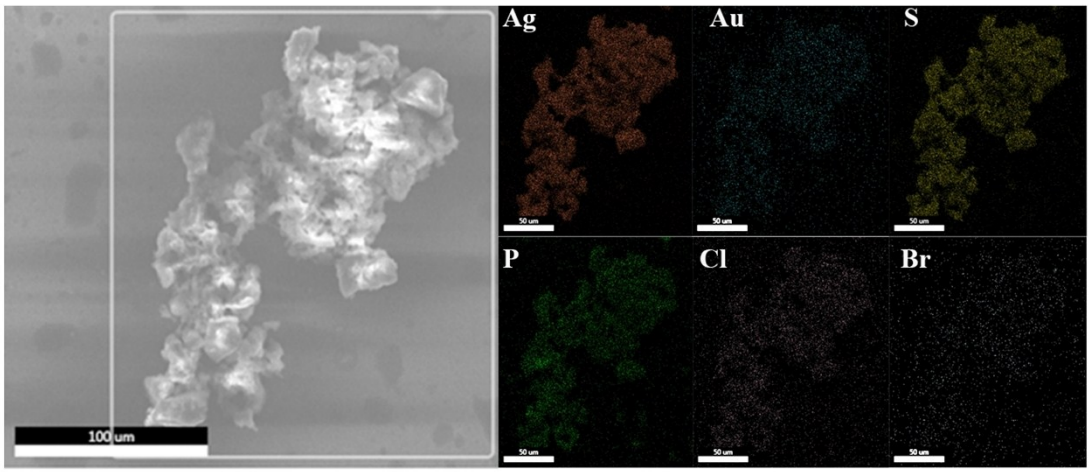

Fig. S6: EDX profile of 1.